



Thermally Oxidized Nanodiamond: An Effective Sorbent for Separation of Methotrexate from Aqueous Media: Synthesis, Characterization, In Vivo and In Vitro Biocompatibility Study

Mostafa Zamani^{1,2} · Mozghan Aghajanzadeh^{1,2} · Hossein Molavi³ · Hossein Danafar^{4,5,6} · Akbar Shojaei⁷

Received: 26 August 2018 / Accepted: 5 December 2018 / Published online: 7 December 2018
© Springer Science+Business Media, LLC, part of Springer Nature 2018

Abstract

In the present study the effect of nanodiamond (ND) on the adsorption capacity of Drug has been investigated. Thermal oxidation nanodiamond (OND) was used as adsorbents for Methotrexate adsorption. The surface properties of NDs were studied by Fourier transform infrared spectroscopy and zeta potential. It was determined that thermal oxidation changed the surface properties of ND, including increase the amount of carboxylic acid groups and decreasing the zeta potential of ND by increasing the thermal oxidation time. The adsorption experiments showed that untreated ND (UND) has large adsorption capacity and fast adsorption kinetic for methotrexate (MTX). These results suggest that the adsorption behavior of UND with the MTX follows not only the charge but also the chemical interaction. Due to form the strong hydrogen bond between the carboxyl groups of MTX and the oxygen containing groups on the surface of NDs, Kinetic studies showed that the kinetic data are well fitted with the pseudo- second-order model for most of the adsorbents. MTT assay, Hemolysis assay and acute toxicity were used for determining biocompatibility of the adsorbents; MTT assay showed no significant toxicity up to near 300 µg/mL, OND showed neglectable hemolysis and acute toxicity result demonstrated OND was nontoxic.

Keywords Nanodiamond · Drug adsorption · Biocompatibility · Methotrexate

Electronic supplementary material The online version of this article (<https://doi.org/10.1007/s10904-018-1043-0>) contains supplementary material, which is available to authorized users.

✉ Hossein Danafar
danafar@zums.ac.ir

✉ Akbar Shojaei
akbar.shojaei@sharif.edu

- ¹ Student Research Center, Zanjan University of Medical Sciences, Zanjan, Iran
- ² Department of Pharmaceutical Biomaterials, School of Pharmacy, Zanjan University of Medical Sciences, Zanjan, Iran
- ³ Institute for Nanoscience and Nanotechnology (INST), Sharif University of Technology, Tehran, Iran
- ⁴ Zanjan Pharmaceutical Nanotechnology Research Center, Zanjan University of Medical Sciences, Zanjan, Iran
- ⁵ Department of Medicinal Chemistry, School of Pharmacy, Zanjan University of Medical Sciences, Zanjan, Iran
- ⁶ Cancer Gene Therapy Research Center, Zanjan University of Medical Sciences, Zanjan, Iran
- ⁷ Department of Chemical and Petroleum Engineering, Sharif University of Technology, Tehran, Iran

1 Introduction

In 2010, approximately 40,000 people died due to drug poisoning and drug overdosing (accidental and intentional) in the United States. In other words, the rate of drug overdose-related mortality has increased from 6.1 per 100,000 standard population in 1999 to 16.3 in 2015 [1], an overall, it grows by 5.5% each year. Intentional self-harm and accidental death due to drug abuse or overdosing is very common in the Western world. Today, because of an increase in the number of prescriptive drugs with high risk factors, their toxicity is more prevalent than in the past [2]. So today researcher are looking for a better solution for overcoming this problem. Some of these solutions are, specific fast-acting antidotes and adsorbents that can be effective in treating and caring poisoned patients in emergency situations if they are used at the appropriate time. They can limit mortality. In 2015, antidotes and adsorbent were used 184,742 times in US. But if they are used incorrectly, they can be harmful for patients [3–6].

Methotrexate is primarily known as an anti-neoplastic anti-metabolite with immunosuppressant properties that

interferes with the actions of folate in cellular synthesis, and in excess this action results in cell death. However, methotrexate has some important adverse effects, for example, it can cause gastrointestinal tract, bone marrow and kidneys toxicity and sometimes high dose intravenous therapy or intrathecal administration, can cause severe toxicity of central nervous system (CNS) [7]. So, in some cases, it should be necessary to use adsorbents and antidotes to improve the patient's condition and even save them. There are some adsorbents and antidotes such as liposomes [8], lipid emulsions [9], polycations [10], polymeric nanoparticles [11], modified cyclodextrins and related compounds [12], enzymes [13], oligonucleotides [14], antibodies and recombinant proteins [15], metal–organic frameworks (MOFs) [16], activated carbon [17], nanodiamond (ND) [18, 19], etc.

Among these materials, ND is used as a relatively new adsorbent agent. NDs due to lack of toxicity, high resistance and acceptable chemical stability against harsh conditions and high affinity to organic molecules, are useful materials for adsorption. ND in comparison to graphene, carbon nanotube and other carbon-based nanoparticles, has a high surface reactivity because of specific surface area about 200 m²/g that could be easily functionalized with appropriate polar groups [20, 21] such as carbonyl (ketone, ester or aldehyde), carboxyl, different type of alcohols and ether groups are the main surface functional groups on raw ND.

Carboxyl group is one of the acceptable and possible functional groups on the ND surface [22–24]. So, to create a layer of carboxylic group on the surface of ND, some methods such as chemical and thermal oxidation have been used [25]. This method can efficiently make a homogeneous layer of carboxyl groups on the ND surface.

In present study, we evaluate the effect of surface charge of ND on the adsorption capacity of drugs. For this purpose, thermally oxidized ND was used as adsorbents and the adsorption capacity of all NDs was investigated. The focus was on acute overdose, rather than treating iatrogenic (such as side effects) toxicity, such as intravenous methotrexate in cancer chemotherapy.

2 Experimental

2.1 Materials and Methods

Detonated ND with an average particle diameter of 4–6 nm, purity of 98–99% and specific surface area of 282 m²/g was purchased from NaBond Technologies Co., China, MTX (Aldrich, St. Louis, USA, USA), Trypan blue dye and 5-(Dimethylthiazol-z-yl)-2,5-diphenyltetrazolium bromide (MTT) were purchased from Sigma. All other agents and solvents used in this study were analytical grade and all solutions were prepared with distilled and double distilled water.

2.2 Thermal Oxidation of ND

To create a homogeneous layer of carboxyl group on the surface of ND, as-received ND was oxidized at 425 °C for 4.5 h under air atmosphere according to reported procedure [26–28].

2.3 Characterization

Fourier transform infrared (FTIR) spectroscopy analysis was carried out using 100-FT-IR Spectrometer, Perkin-Elmer, with a wavenumber resolution of 4 cm⁻¹ to characterize the surface chemistry of different NDs, and illustrate the interaction between MTX and NDs. The zeta potential of different NDs in ultrapure water was measured by a zeta potential analyzer (Zetasizer, Malvern Instruments, Worcestershire, UK, model Nano ZS). Field emission scanning electron microscopy (FESEM–MIRA3 TESCAN) was used to determine the morphology of the NDs. X-ray diffraction (XRD) patterns were obtained at room temperature using a X-pert Philips, pw 3040/60 diffractometer with a copper anode and a graphite monochromator to select Cu K_{α1} radiation ($\lambda = 1.54060 \text{ \AA}$), and with accelerating voltage and current of 40 kV and 40 mA, respectively. TEM image was recorded on a Philips CM 120 transmission electron microscope at an accelerating voltage of 120 KV.

2.4 In Vivo and In Vitro Biocompatibility Test of Adsorbent (ND)

2.4.1 Cell Cytotoxicity Assay

MTT assay was used for determining toxicity of synthesized adsorbent, for this purpose, Human embryonic kidney cells 293 (HEK-293) were cultured according to previous works [29, 30], the cells were incubated at 37 °C in 5% CO₂ atmosphere. Then, cells were seeded in 96-well plates at a density of 5000 cells per well, and grown for 24 (for HEK-293). The cells were then incubated with a series of UND and OND-4.5 loaded micelles in different concentrations for 72 h. then medium was removed and fresh DMEM medium (0.1 mL) and 0.01 mL of MTT solution (5 mg/mL) were added to each well. Then the plates were incubated in 5% CO₂ at 37 °C for another 4 h. After incubation, for dissolving formazan crystals, the culture medium was taken out and 0.05 mL of DMSO was added to each well and left for 10 min at room temperature. The absorbance was measured at a wavelength of 570 nm using a plate reader (Tecan Infinite 500). Three replicates were conducted for each experiment.

2.4.2 Hemolysis Assay

For determining Hemolytic activity of UND and OND-4.5 fresh human blood obtained from a volunteer was diluted by physiological saline, then red blood cells (RBC) were separated from serum using centrifugation (4000 rpm, 5 min). After separation, RBCs were washed with isotonic Phosphate Buffer Saline (PBS). Then RBCs suspension was diluted with PBS to reach appropriate concentration [31, 32]. After dilution, RBCs were mixed with NDs solution (10 mg/mL), after mixing, RBCs were incubated at 37 °C in a shaker incubator for 4 h. For negative and positive controls we used PBS and deionized respectively. Then, the tube containing RBCs were centrifuged at 13,000 rpm for 10 min, then 100 μ L of supernatant of each sample was transferred to a 96-well plate. Bio-Rad 680 microplate reader was used for measuring free hemoglobin at wave length 540 nm. The hemolysis ratio (HR) of RBCs was determined using the following formula: $\text{hemolysis (\%)} = (A_{\text{ND}} - A_{\text{negative}}) / (A_{\text{positive}} - A_{\text{negative}}) \times 100$, where A_{ND} , A_{negative} and A_{positive} were denoted as the adsorption of ND treated RBCs, negative and positive controls, respectively. All hemolysis experiments were performed in triplicates.

2.4.3 Acute Toxicity

For determining acute toxicity of adsorbent, first, according to ideal laboratory environment (OCED), 10 Adult mice (30–35 g) were selected from laboratory of Zanjan University of Medical Sciences in both sexes and every 5 mice were placed in a cage for seven days. Experimental protocol and morally were confirmed by University's Research and Ethics Committee. After experiment the all animals were sacrificed. Acute toxicity test was carried out according to OCED protocols [33], briefly, animals were treated orally with different doses (control, 17.5, 175, 1750, 5000 mg/kg). Animals were weighed before administration and after 24 h and 168 h. Any physical activities and behavioral changes of animals were observed for 6 h after the administration of the dose. After surviving all the animals during 24 h, two additional animals were treated at the highest dose, if these animals survived, the acute toxicity is more than the limit dose and the test is stopped.

2.5 Batch Adsorption Experiments

The calibration curve of MTX was prepared by measuring the characteristic absorbance of MTX in a series of standard solution (1–5 mg/L) at 306 nm. Then the initial and equilibrium concentrations of MTX were calculated using this calibration curve. 20 mg of different NDs were dispersed in 50 mL of MTX solution at different concentrations (0.24–0.96 mg/mL), then the solution was stirred at

room temperature with a magnetic stirrer for 2 h. At specified time intervals, the NDs were separated from the MTX solution with centrifugation at 20,000 rpm for 15 min, and the residual concentration of MTX was determined using the UV–Vis spectroscopy. The equilibrium adsorption capacity (q_e) was calculated according to the following Eq. (1) [16]:

$$q_e = \frac{(C_0 - C_e)V}{W} \quad (1)$$

where C_0 and C_e (mg/L) are the initial and equilibrium concentrations of MTX, respectively, V (L) is the volume of the drug solution and W (g) is the initial mass of the NDs. Each batch adsorption experiment was repeated at least twice to check the repeatability of the data.

2.6 Adsorption Kinetic Study

For determining kinetic of adsorption, exactly 5 mg of each adsorbents were added into a series of 15 mL Conical Centrifuge Tubes containing 10 mL of 100 μ g/mL MTX. The tubes were shaken at 300 rpm at 310 K, and at predetermined time interval one tube was taken and centrifuged at 4000 rpm and 1 mL of supernatant was collected. The concentrations of non-adsorbed MTX were analyzed by UV–Vis at 307 nm.

2.7 Statistical Analysis

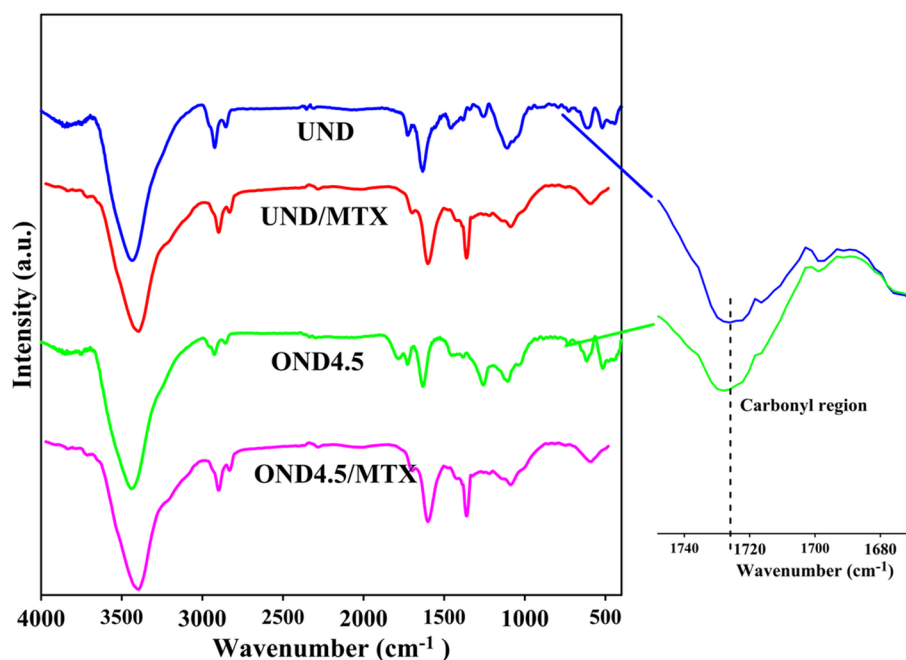
The experiments were repeated at least three times, and the data were expressed as means \pm SD. Comparisons between groups were made with ANOVA. If ANOVA analysis indicated significant differences, a Sidak test was performed to compare mean values between treatments.

3 Results and Discussion

3.1 FT-IR Analysis

To investigate the effect of thermal oxidation on the surface chemistry of NDs, FTIR analysis was conducted on UND and OND-4.5. As shown in Fig. 1, the sharp peaks in the range of 1000–1200 cm^{-1} appeared in the spectra of NDs, which could be due to the stretching vibration of different C–O–C groups, and the intensity of these peaks increased after oxidation. The bands observed at 1650–1750 cm^{-1} are assigned to the stretching vibration of different carbonyl groups which are on the surface of NDs. The small bands appeared around 2850–3050 cm^{-1} are assigned to the C–H stretching vibration of saturated and unsaturated carbons [34, 35]. Moreover, the broad absorption band observed in the range of 3200–3600 cm^{-1} could be due to the formation

Fig. 1 FTIR spectra of all NDs before and after adsorbing MTX



of hydrogen bond between carbonyl and hydroxyl groups of NDs.

As can be inferred from Fig. 1, the characteristic band of carboxylic group appeared around 1723 cm^{-1} is shifted to higher frequencies and becomes more intensified after thermal oxidation. This result suggest that, the content of carboxylic acid group on the surface of ND increased after thermal oxidation which is similar to the results reported by other researchers [36].

To investigate the possible interactions between NDs and MTX, the FTIR spectra of NDs is compared with that of NDs/MTX in Fig. 1. As can be inferred from this Figure, some differences are observed between the spectra of the nanoparticles before and after adsorbing MTX. It can be seen that there is an absorption band around $2850\text{--}2950\text{ cm}^{-1}$, which is assigned to the CH stretching vibration of adsorbed MTX. The peak of carbonyl group, is shifted to lower frequencies after adsorbing MTX, which could be attributed to formation of hydrogen bond between carbonyl and hydroxyl groups of NDs and polar functional groups of MTX. The hydrogen bonding are obviously improved by increasing the number of polar functional groups on the surface of ND, which could be demonstrated by the redshift of carbonyl peak of OND-4.5. Moreover, in the spectrum of NDs/MTX, there are two sharp absorption bands around 1400 cm^{-1} and 1600 cm^{-1} which are assigned to the aromatic ring of the adsorbed MTX on the surface of NDs. Additionally, the strong and broad absorption band observed in the range of $3200\text{--}3600\text{ cm}^{-1}$ could be due to the formation of hydrogen bonds between the oxygen containing groups of NDs and the polar groups of MTX. These results indicate that MTX is

successfully adsorbed on the surface of NDs. Additionally, the amide bonds within the MTX structure overlapped with the carboxyl groups on the surface of NDs, which resulting to increase the intensity of this band in the spectrum of MTX adsorbed NDs [37].

3.2 XRD Analysis

The powder XRD patterns of UND and OND-4.5 are given in Fig. 2. The main characteristic peaks of UND ($2\theta = 21.5, 43.2$ and 74.8°) well match with the previously

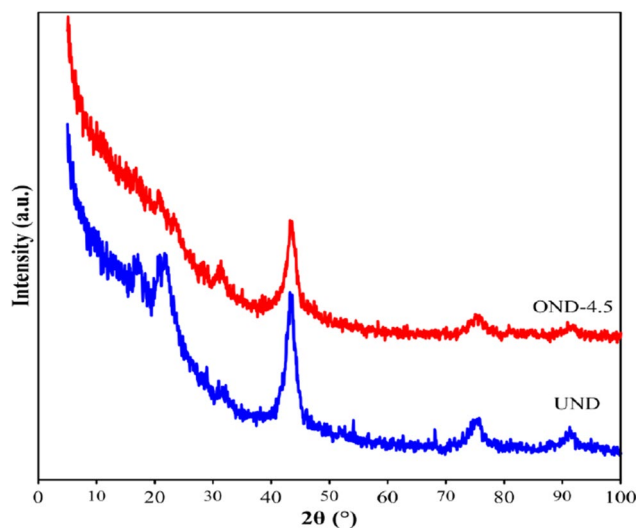


Fig. 2 XRD patterns of UND and OND-4.5

reported diffraction peaks in literature [38, 39]. In the XRD pattern of UND the broad peak observed at $2\theta = 21.5^\circ$, could be attributed to the reflection from a graphite-type lattice [39, 40]. As can be seen from Fig. 2, the position of this peak shift to lower degrees and the intensity of that decrease after thermal oxidation, which indicates that thermal oxidation, decrease the graphite-type lattice of ND. The other characteristic peaks observed in the XRD patterns of UND and OND-4.5, such as $2\theta = 43.2$ and 74.8° , are correspond to the (111) and (220) reflection from a diamond-type lattice, respectively. The position and also the intensity of these peaks do not changed after thermal oxidation, which indicates that thermal oxidation does not affect the core diamond-type lattice of ND [39].

3.3 Particle Morphology

In order to investigate the particle size and the size distribution of NDs, FESEM analysis were performed on UND and OND-4.5. To give good FESEM images, the ND suspensions in water were dispersed onto Si wafers (were precleared with piranha acid solution) and imaged at medium resolution. As shown in Fig. 3a, b, ND particles have a spherical crystal structure with a characteristic size of about 20–40 nm. Some agglomeration centers with maximum sizes of about 500 nm were also observed in the FESEM images of these nanoparticles. FESEM image of OND-4.5 shows no change in the nanoparticle morphology, which confirms that ND is stable after oxidation at this condition [38, 41]. The particle size and morphology of OND-4.5 was also investigated using TEM image. Figure 3c illustrates that OND-4.5 particles have a spherical shape.

3.4 Zeta Potential of Adsorbent

The zeta potential of the aqueous suspension of NCs were also measured. Zeta potential for OND 4.5 determined in the PBS buffer solution at pH 7.4. Zeta potential of adsorbent at pH 7.4 were found to be about -9.65 ± 0.57 mv. It is clear that at the pH 7.4 where our results showed a negative zeta potential due to carboxyl group of oxidized nanodiamond. Therefore, as we knew, higher oxygen content can cause to more electrostatic affinity to the drugs. So, when oxygen content of nanodiamond were increased, the adsorption ability were increased. Therefore with this method, we can improve adsorption capacity of nanodiamond.

3.5 In Vivo and In Vitro Biocompatibility Test of Adsorbent (ND)

3.5.1 Cell Cytotoxicity Assay

The biocompatibility studies using HEK-293 cells revealed that UND and OND-4.5 was nontoxic up to the highest testing concentration of 280 $\mu\text{g}/\text{mL}$ (Fig. 4), indicating its biocompatibility. Both of adsorbent approximately have same cell viability, so in this project due to great adsorption capacity of NDs, NDs biocompatibility up to near 300 $\mu\text{g}/\text{mL}$ is very good for our purpose to adsorbing drugs.

3.5.2 Hemolysis Assay

Because the application of the adsorbent in the pharmaceutical field counts on several aspects including safety. Therefore, a hemolysis assay was performed based on the previous report [32]. As shown in Table 1 OND-4.5 showed negligible hemolysis toxicity (2.47%) to RBCs even at adsorbent concentration of 10 mg/mL , indicating the great blood compatibility of modified OND-4.5 and the potential

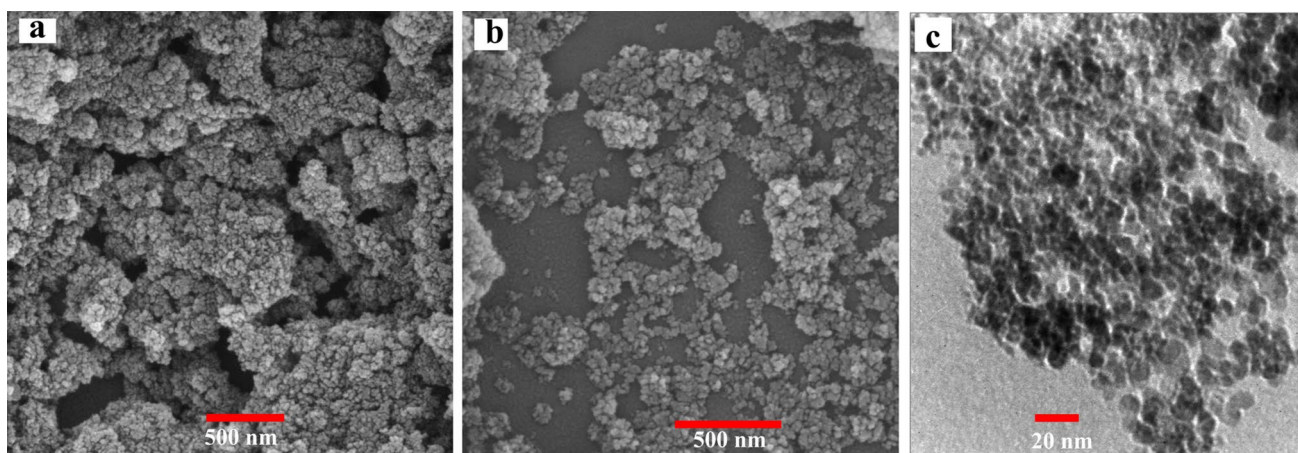


Fig. 3 FESEM images of UND (a) and OND-4.5 (b), and the TEM image of OND-4.5 (c)

Fig. 4 Cell viability of UND and OND-4.5. (HEK-293)

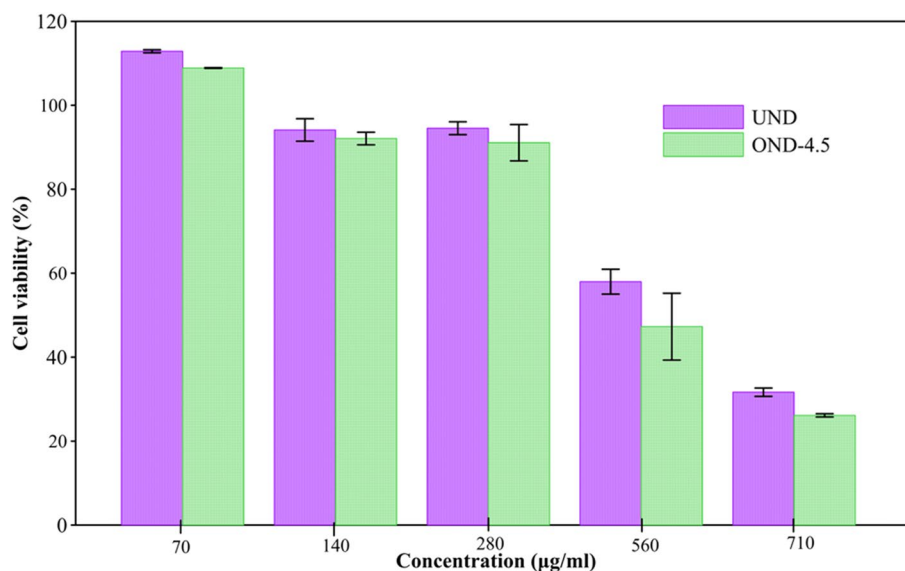


Table 1 Hemolysis percent of UND and OND 4.5

Sample	Concentration (mg/mL)	Hemolysis (%)
UND	10	35.63 ± 6.07
OND-4.5	10	2.47 ± 2.78

application as drug adsorbent. But, UND have hemolysis toxicity about 35.63%. The increase could be justified in terms of zeta potential of NCs. the neutral zeta potential of OND changed to more negative when the carbocyclic group added to UND [36]; therefore, due to negative surface charge of cells [42] the interaction between the OND and cell walls decreased. So, it was expected that, percent of hemolysis for OND decreased to 2.47%, but, because of high interaction between UND and cell walls, the destruction of RBCs by UND could increase and the hemolysis of UND reach to 35.63%. So in order to these results, modification of UND reduce its toxicity. Therefore, it can be concluded OND-4.5 is suitable adsorbent for drugs adsorption. Figure 5 shows schematic comparison between NDs and positive control.

3.5.3 Acute Toxicity

For acute toxicity test we treated mice with a range of doses. Mice which treated with 5000 mg/Kg are showed in Fig. 6. As it demonstrates, after 168 h (one week), none of our mice are died at 2000 mg/kg. So due to OCED and Hodge and Sterner scale we deduced that all of our adsorbent are practically none toxic [33]. In Addition, body weight change is an important indicator for potential toxicity of formulation. Table 2 demonstrates weight change in mice after 24 and 168 h, as it demonstrates any increase in mice weight were natural.

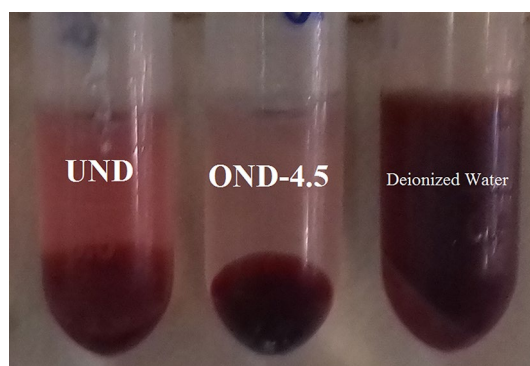


Fig. 5 Schematic comparison between NDs and control

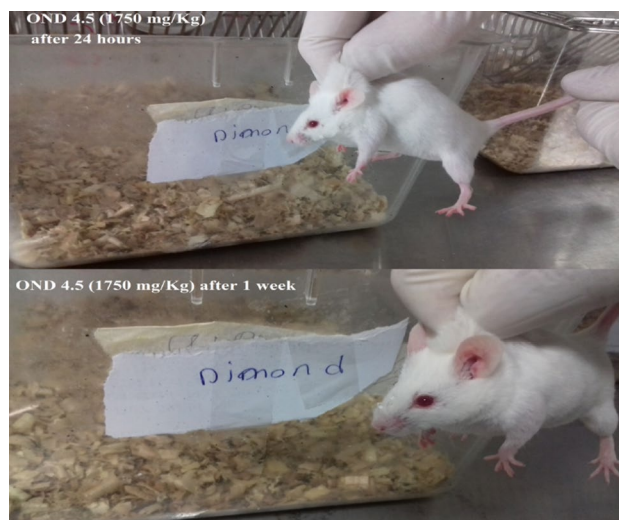


Fig. 6 Illustration of treated mice after predetermined time

Table 2 Weight change of NDs treated mice

Single oral dose	Weight changes after 24 h (%)	Weight changes after a week (%)
	NDH 4.5	NDH 4.5
Control	1.00 ± 1.80	1.98 ± 1.80
17.5	3.09 ± 1.79	4.12 ± 1.79
175	5.15 ± 0.00	7.22 ± 1.79
2000	1.96 ± 1.79	3.92 ± 1.70
5000	Dead	Dead

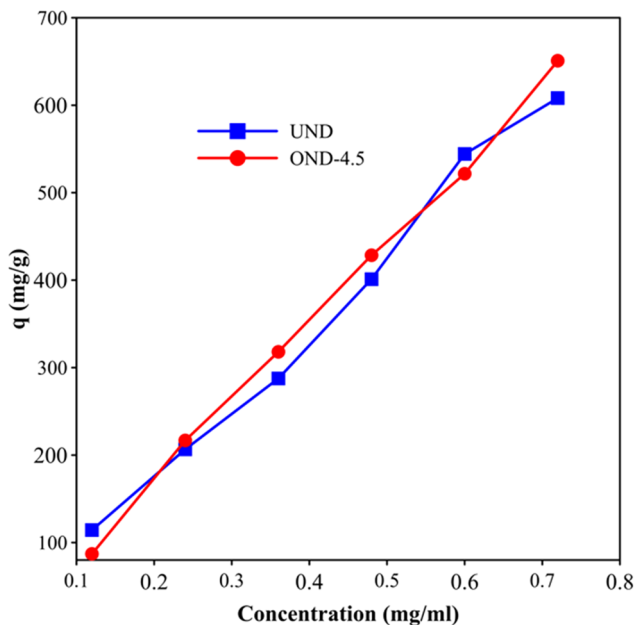


Fig. 7 Drug adsorption curve for UND and OND-4.5

3.6 Adsorption Study of ND

The adsorption capacity of MTX was measured via putting UND and OND in MTX aqueous solution. Residual drug concentrations were evaluated at various time intervals using UV–Vis spectrophotometer (λ_{maxMTX} : 307 nm). In order to optimize the effect of Drug/NDs ratio on adsorption efficiency, a variety of MTX/NDs mass ratios in feed were studied. As shown in Fig. 7, when mass ratio of MTX/NDs were increased, the adsorption efficiency of NDs were increased. According to this experiment, the maximum adsorption efficiency was in mass ratio=0.72. This showed, NDs can adsorb more drugs at high concentrations of drugs. As shown in Fig. 7, approximately the adsorption efficiency of UND and OND was similar. The maximum adsorption capacities of OND and UND were about 650.82 and 604.18 mg/g, respectively. As it can be seen, the adsorption capacity of oxidized ND is slightly higher than un-oxidized ND, this phenomenon could be justified

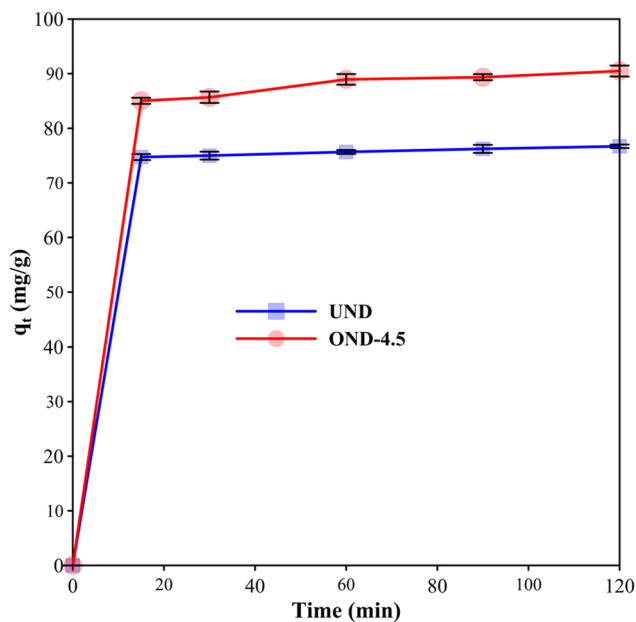


Fig. 8 Effect of contact time on adsorption rate

Table 3 Kinetic parameters for the adsorption of MTX on NDs at 37 °C and initial concentration of 100 µg/mL

Adsorbent	q_e (mg/g)	k_2 (g/mg/min)	R^2	
			First-order	Second-order
UND	604.18	$1.04 \cdot 10^{-2}$	~ 1.000	0.645
OND 4.5	650.82	$5.23 \cdot 10^{-3}$	0.999	0.742

due to the fact that by increasing the functional groups, the interaction forces between adsorbent and Drugs like electrostatic force and hydrogen bond were increased. Therefore, the adsorption capacity were increased too.

3.7 Kinetic Study

The Drug removal rate was calculated on the basis of pervious works [16]. Figure 8 shows drug removal rate vs. time is plotted for the two type of NDs. within approximately 15 min the removal rate of MTX by NDs reach a constant amount, indicating the effectiveness of NDs adsorbents. The kinetic experiments of NDs adsorption were carried out with the results for MTX (Table 3). To study of adsorption mechanism, classical kinetic models were used to show the mechanism of NDs adsorption as follows:

Equation (2) represent pseudo-first-order model:

$$\ln(q_e - q_t) = \ln(q_e) - K_1 t \tag{2}$$

Equation (3) represent pseudo-second-order model:

$$\frac{t}{q_t} = \frac{1}{K_2 q_e^2} + \frac{t}{q_e} \tag{3}$$

In these equation, q_e and q_t represent the amount of MTX that was adsorbed (mg/g) at equilibrium and time t , respectively, and the K_1 and K_2 show the kinetic rate constants 50 and 51, respectively. The kinetic results (Table 3) well characterized via pseudo-second-order model with good correlation coefficients ($R^2 > 0.995$). Also, good recovery and stability are expected and good for the large-scale applications of adsorbents. In addition, as we expected, the removal rate of OND 4.5 was higher than UND. It indicated that, thermal oxidation was useful for increasing adsorption ability of NDs.

4 Conclusion

In this study, NDs capacity for removing MTX has been studied in details. The OND 4.5 is also reusable and easily recycled several times in adsorption of drugs. In other words, the MTX removal or adsorption application of modified oxidized NDs were investigated. Kinetic study showed the adsorbance capacity reach to maximum within 15 min due to great affinity between MTX and NDs. In order to investigate biocompatibility of NDs several test like: MTT assay, hemolysis assay and acute toxicity were carried out. MTT assay results revealed that OND 4.5 showed no significant toxicity even at 280 $\mu\text{g/mL}$. Also, OND 4.5 showed neglectable hemolysis percent (2.47%). Therefore, All of those tests showed, OND 4.5 has not significant cytotoxic and categorized as practically nontoxic material.

Acknowledgements This study was supported financially by Zanjan University of medical science (Grant No. A-12-430-33), and Sharif University of Technology, Iran.

Compliance with Ethical Standards

Conflict of interest The authors declare that they have no conflict of interest.

References

1. V. Forster, J.-C. Leroux, Nano-antidotes for drug overdose and poisoning. *Sci. Transl. Med.* **7**(290), 290ps14–290ps14 (2015)
2. H. Hedegaard, M. Warner, A.M. Miniño, Drug overdose deaths in the United States, 1999–2015: US Department of Health and Human Services, Centers for Disease Control and Prevention, National Center for Health Statistics (2017)
3. R.C. Dart, L.R. Goldfrank, B.L. Erstad, D.T. Huang, K.H. Todd, J. Weitz et al., Expert consensus guidelines for stocking of antidotes in hospitals that provide emergency care. *Ann. Emerg. Med.* **54**(3), 386–394 (2017)
4. S. Glund, V. Moschetti, S. Norris, J. Stangier, M. Schmohl, J. van Ryn et al., A randomised study in healthy volunteers to investigate the safety, tolerability and pharmacokinetics of idarucizumab, a specific antidote to dabigatran. *Thromb. Haemost.* **114**(05), 943–951 (2015)
5. V. Paget, J. Sergent, R. Grall, S. Altmeyer-Morel, H. Girard, T. Petit et al., Carboxylated nanodiamonds are neither cytotoxic nor genotoxic on liver, kidney, intestine and lung human cell lines. *Nanotoxicology* **8**(sup1), 46–56 (2014)
6. V. Vaijayanthimala, Y.-K. Tzeng, H.-C. Chang, C.-L. Li, The biocompatibility of fluorescent nanodiamonds and their mechanism of cellular uptake. *Nanotechnology* **20**(42), 425103 (2009)
7. A. Coleman, M. Nankoo, Acute kidney injury secondary to the use of methotrexate. *J. Kidney Care* **2**(2), 76–81 (2017)
8. A.B. Dhanikula, D. Lamontagne, J.-C. Leroux, Rescue of amitriptyline-intoxicated hearts with nanosized vesicles. *Cardiovasc. Res.* **74**(3), 480–486 (2007)
9. M.R. Fettiplace, K. Lis, R. Ripper, K. Kowal, A. Pichurko, D. Vitello et al., Multi-modal contributions to detoxification of acute pharmacotoxicity by a triglyceride micro-emulsion. *J. Controll. Release* **198**, 62–70 (2015)
10. R.A. Sheno, M.T. Kalathottukaren, R.J. Travers, B.F. Lai, A.L. Creagh, D. Lange et al., Affinity-based design of a synthetic universal reversal agent for heparin anticoagulants. *Sci. Transl. Med.* **6**(260), 260ra150–260ra150 (2014)
11. C.-M.J. Hu, R.H. Fang, J. Copp, B.T. Luk, L. Zhang, A biomimetic nanosponge that absorbs pore-forming toxins. *Nat. Nanotechnol.* **8**(5), 336 (2013)
12. S. Aniskevich, B.J. Leone, S.J. Brull, Sugammadex: a novel approach to reversal of neuromuscular blockade. *Expert Rev. Neurother.* **11**(2), 185–198 (2011)
13. D.G. Ilyushin, I.V. Smirnov, A.A. Belogurov, I.A. Dyachenko, T.I. Zharmukhamedova, T.I. Novozhilova et al., Chemical polysialylation of human recombinant butyrylcholinesterase delivers a long-acting bioscavenger for nerve agents in vivo. *Proc. Natl. Acad. Sci.* **110**(4):1243–1248 (2013)
14. C.P. Rusconi, J.D. Roberts, G.A. Pitoc, S.M. Nimjee, R.R. White, G. Quick Jr. et al., Antidote-mediated control of an anticoagulant aptamer in vivo. *Nat. Biotechnol.* **22**(11), 1423 (2004)
15. R.J. Flanagan, A.L. Jones, Fab antibody fragments. *Drug Saf.* **27**(14), 1115–1133 (2004)
16. H. Molavi, A. Hakimian, A. Shojaei, M. Raeiszadeh, Selective dye adsorption by highly water stable metal-organic framework: Long term stability analysis in aqueous media. *Appl. Surf. Sci.* **445**, 424–436 (2018)
17. R. Baccar, M. Sarrà, J. Bouzid, M. Feki, P. Blázquez, Removal of pharmaceutical compounds by activated carbon prepared from agricultural by-product. *Chem. Eng. J.* **211**, 310–317 (2012)
18. V.N. Mochalin, A. Pentecost, X.-M. Li, I. Neitzel, M. Nelson, C. Wei et al., Adsorption of drugs on nanodiamond: toward development of a drug delivery platform. *Mol. Pharm.* **10**(10), 3728–3735 (2013)
19. K.-K. Liu, C.-C. Wang, C.-L. Cheng, J.-I. Chao, Endocytic carboxylated nanodiamond for the labeling and tracking of cell division and differentiation in cancer and stem cells. *Biomaterials* **30**(26), 4249–4259 (2009)
20. F. Hajiali, A. Shojaei, Silane functionalization of nanodiamond for polymer nanocomposites-effect of degree of silanization. *Colloids Surf. A* **506**, 254–263 (2016)
21. Z. Delavar, A. Shojaei, Enhanced mechanical properties of chitosan/nanodiamond composites by improving interphase using thermal oxidation of nanodiamond. *Carbohydr. Polym.* **167**, 219–228 (2017)
22. A.M. Schrand, S.A.C. Hens, O.A. Shenderova, Nanodiamond particles: properties and perspectives for bioapplications. *Crit. Rev. Solid State Mater. Sci.* **34**(1–2), 18–74 (2009)
23. J. Nunes-Pereira, A. Silva, C. Ribeiro, S. Carabineiro, J. Buijnsters, S. Lanceros-Méndez, Nanodiamonds/poly (vinylidene fluoride) composites for tissue engineering applications. *Compos. B* **111**, 37–44 (2017)

24. A. Zhukov, F. Gareeva, A. Aleksenskii, A.Y. Vul, Surface charge of detonation nanodiamond particles in aqueous solutions of simple 1: 1 Electrolytes. *Colloid J.* **72**(5), 640–646 (2010)
25. A. Krueger, D. Lang, Functionality is key: recent progress in the surface modification of nanodiamond. *Adv. Func. Mater.* **22**(5), 890–906 (2012)
26. P. Karami, A. Shojaei, Morphological and mechanical properties of polyamide 6/nanodiamond composites prepared by melt mixing: effect of surface functionality of nanodiamond. *Polym. Int.* **66**(4), 557–565 (2017)
27. F. Hajiali, A. Shojaei, Network structure and mechanical properties of polydimethylsiloxane filled with nanodiamond—effect of degree of silanization of nanodiamond. *Compos. Sci. Technol.* **142**, 227–234 (2017)
28. F. Liao, X. Zeng, H. Li, X. Lai, F. Zhao, Synthesis and properties of UV curable polyurethane acrylates based on two different hydroxyethyl acrylates. *J. Central South Univ.* **19**(4), 911–917 (2012)
29. V.N. Mochalin, O. Shenderova, D. Ho, Y. Gogotsi, The properties and applications of nanodiamonds. *Nat. Nanotechnol.* **7**(1), 11 (2012)
30. D. Ho, C.-H.K. Wang, E.K.-H. Chow, Nanodiamonds, The intersection of nanotechnology, drug development, and personalized medicine. *Sci. Adv.* **1**(7), e1500439 (2015)
31. M. Zamani, K. Rostamizadeh, H.K. Manjili, H. Danafar, In vitro and in vivo biocompatibility study of folate-lysine-PEG-PCL as nanocarrier for targeted breast cancer drug delivery. *Eur. Polym. J.* **103**, 260–270 (2018)
32. M. Zamani, E. Naderi, M. Aghajanzadeh, M. Naseri, A. Sharafi, H. Danafar, Co1—XZnxFe2O4 based nanocarriers for dual-targeted anticancer drug delivery: synthesis, characterization and in vivo and in vitro biocompatibility study. *J. Mol. Liquids* **274**, 60–67 (2018)
33. O.O. Guideline, 425: acute oral toxicity—up-and-down procedure. OECD Guidel Test. Chem. 2, 6–12 (2001)
34. H. Molavi, F.A. Joukani, A. Shojaei, Ethylenediamine grafting to functionalized NH₂-UiO-66 using green aza-michael addition reaction to improve CO₂/CH₄ adsorption selectivity. *Ind. Eng. Chem. Res.* **57**(20), 7030–7039 (2018)
35. H. Molavi, A. Shojaei, S.A. Mousavi, Improving mixed-matrix membrane performance via PMMA grafting from functionalized NH₂-UiO-66. *J. Mater. Chem. A* **6**(6), 2775–2791 (2018)
36. H. Molavi, A. Shojaei, A. Pourghaderi, Rapid and tunable selective adsorption of dyes using thermally oxidized nanodiamond. *J. Colloid Interface Sci.* **524**, 52–64 (2018)
37. R.A. Hashad, R.A. Ishak, A.S. Geneidi, S. Mansour, Surface functionalization of methotrexate-loaded chitosan nanoparticles with hyaluronic acid/human serum albumin: comparative characterization and in vitro cytotoxicity. *Int. J. Pharm.* **522**(1–2), 128–136 (2017)
38. M. Baidakova, New prospects and frontiers of nanodiamond clusters. *J. Phys. D* **40**(20), 6300 (2007)
39. A. Aleksenskii, M. Baidakova, A.Y. Vul, V. Siklitskii, The structure of diamond nanoclusters. *Phys. Solid State* **41**(4), 668–671 (1999)
40. E.A. Feijani, A. Tavassoli, H. Mahdavi, H. Molavi, Effective gas separation through graphene oxide containing mixed matrix membranes. *J. Appl. Polym. Sci.* **135**(21), 46271 (2018)
41. M. Shalaginov, G. Naik, S. Ishii, M. Slipchenko, A. Boltasseva, J.-X. Cheng et al., Characterization of nanodiamonds for metamaterial applications. *Appl. Phys. B* **105**(2), 191 (2011)
42. D. Haydon, The surface charge of cells and some other small particles as indicated by electrophoresis: I. The zeta potential-surface charge relationships. *Biochem. Biophys. Acta* **50**(3), 450–457 (1961)